RSC Advances

ROYAL SOCIETY OF CHEMISTRY

www.rsc.org/advances

Equilibrium and kinetic studies of Se(VI) removal by Mg-Al layered double hydroxide doped with Fe^{2+}

Tomohito Kameda*, Eisuke Kondo, Toshiaki Yoshioka

Graduate School of Environmental Studies, Tohoku University, 6-6-07 Aoba, Aramaki, Aoba-ku, Sendai 980-8579, Japan

*Corresponding author

Tel: +81-22-795-7212; Fax: +81-22-795-7212

E-mail: kameda@env.che.tohoku.ac.jp

Abstract[1]

Mg-Al layered double hydroxide (Mg-Al LDH) doped with Fe^{2+} was found to be superior to undoped Mg-Al LDH in the removal of Se(VI) from aqueous solutions. For both systems, Se(VI) as SeO_4^{2-} was removed through anion exchange with intercalated Cl^-. In the Fe^{2+}-doped Mg-Al LDH, however, some of the Se(VI) was reduced to Se(IV) upon oxidation of Fe^{2+} to Fe^{3+} in the LDH host layer to produce SeO_3^{2-}, which was also adsorbed by the Fe^{2+}-doped Mg-Al LDH through anion exchange. The reduction of Se(VI) to Se(IV) is advantageous for Se(VI) removal by Fe^{2+}-doped Mg-Al LDH due to the larger charge density of SeO_3^{2-}. The Fe^{2+}-doped Mg-Al LDH effectively removed Se(VI) from an aqueous solution because of the anion exchange properties of Mg-Al LDH and activity of Fe^{2+} as a reducing agent. Se(VI) removal occurs through Langmuir-type adsorption, where the maximum adsorption and equilibrium adsorption constant were 1.4 mmol g^{-1} and 1.6, respectively. Se(VI) removal is well expressed as a pseudo second-order reaction. The apparent rate constants at 10, 30, and 60 °C were 1.2×10^{-3}, 1.5×10^{-3}, and 2.2×10^{-3} g $mmol^{-1}$ min^{-1}, respectively, and the apparent activation

---

[1] Mg-Al LDH, Mg-Al layered double hydroxide; XRD, X-ray diffraction; XPS, X-ray photoelectron spectroscopy

energy was 10.0 kJ mol^{-1}. The rate-determining step is chemical adsorption through anion exchange of SeO_4^{2-} and SeO_3^{2-} with intercalated Cl^-.

Introduction

Layered double hydroxides (LDHs) are typically represented by the formula $[M^{2+}_{1-x}M^{3+}_{x}(OH)_2](A^{n-})_{x/n}\bullet mH_2O$, where M^{2+} and M^{3+} are divalent and trivalent metal ions, respectively; x denotes the $M^{3+}/(M^{2+} + M^{3+})$ molar ratio ($0.20 \leq x \leq 0.33$); and A^{n-} is, for example, CO_3^{2-} or Cl^-.[1-4] An LDH consists of stacked M^{3+}-bearing brucite-like octahedral layers, where some of the M^{3+} is replaced by M^{2+}, in which the charge of the positive layer is electrically neutralized by interlayer anions. The interlayer space is occupied by water molecules in the hydration shell of these intercalated anions. LDHs have been investigated as promising materials for water preservation and purification. For example, LDHs can adsorb oxometalates such as arsenite, arsenate, chromate, selenite, and selenate from aqueous solutions.[5–13] We have also examined the removal of antimonate using LDHs.[14–16] On the other hand, magnetic chitosan composites are known to be a novel material that exhibits good sorption behavior toward various toxic metal in aqueous solution.[17]

In our recent study, a Mg-Al LDH doped with Fe^{2+} was prepared by co-precipitation, where some Mg^{2+} ions in the LDH host layer were replaced with Fe^{2+}, and used to remove Cr(VI) from an aqueous solution through anion exchange.[18] Cr(VI) was reduced to Cr(III) upon the oxidation of Fe^{2+} to Fe^{3+}, and the resultant Cr(III) combined with OH^- to produce $Cr(OH)_3$. In this study, the Fe^{2+}-doped Mg-Al LDH was applied to the removal of Se(VI) from aqueous solutions, as Se also forms toxic compounds. Se commonly exists as Se(VI) and Se(IV) in aqueous solutions. Although Se was added as one of harmful substances in the effluent standards in Japan in 2001, the treatment method of Se wastewater is not established sufficiently. New treatment method for Se wastewater must be developed. While Se(IV) can be removed by co-precipitation with Fe(III),[19] similar treatment of Se(VI) is difficult due to its high stability in aqueous solutions. In general, for adsorption method, activated carbon is known to be less effective for the removal of Se(VI) and Se(IV). Activated alumina is known to be less effective for the removal of Se(VI), although it is effective for the removal of Se(IV). However, the Fe^{2+}-doped Mg-Al LDH can adsorb Se(VI) from an aqueous solution and reduce Se(VI) to Se(IV), which is advantageous for its removal to be adsorbed. Furthermore, equilibrium and kinetic studies were conducted to determine the properties of Se(VI) removal by the Fe^{2+}-doped Mg-Al LDH.

Experimental methods

Fe^{2+}-doped Mg-Al LDH was prepared through the dropwise addition of a Mg-Fe-Al chloride solution to a NaOH solution at a constant pH, as reported in our previous paper.[18] The Fe^{2+}-doped Mg-Al LDH contained 16.6 wt% Mg^{2+}, 6.3 wt% Al^{3+}, 8.7 wt% Fe^{2+}, and 4.4 wt% Fe^{3+}. An undoped Mg-Al LDH was also prepared through the dropwise addition of a Mg-Al chloride solution to a NaOH solution at a constant pH, and it contained 25.0 wt% Mg^{2+} and 6.8 wt% Al^{3+}.

An aqueous Se(VI) solution containing SeO_4^{2-} ions was prepared by dissolving Na_2SeO_4 in deionized water. The Fe^{2+}-doped Mg-Al LDH and undoped Mg-Al LDH were added to 500 mL of 1 mM Se(VI) solution, and the resultant suspension was stirred at 10–60 °C for 120 min, with continuous N_2 bubbling. Samples of the suspension were collected at different time intervals and immediately filtered through a 0.45 μm membrane filter. The filtrates were analyzed for residual Se. In order to determine the adsorption isotherm of Se(VI) adsorbed by the Fe^{2+}-doped Mg-Al LDH, 20 mL of 0.5–25 mM Se(VI) solution and 0.2 g of Fe^{2+}-doped Mg-Al LDH were placed in 50 mL screw-top tubes and shaken at 30 °C for 24 h.

The two types of LDHs before and after removal of Se(VI) were analyzed by X-ray diffraction (XRD) using Cu Kα radiation. The Fe^{2+}-doped Mg-Al LDH after removal of Se(VI) was dissolved in 1 M HCl, and the Fe^{2+} concentration was determined by performing UV-Vis spectroscopy at 510 nm using the phenanthroline method. Furthermore, the oxidation state of Se in the LDH after removal of Se(VI) was investigated using X-ray photoelectron spectroscopy (XPS). For the adsorption experiments, the residual concentration of Se in the filtrates was determined using inductively coupled plasma-atomic emission spectrometry (ICP-AES), with an error of 0.1 mg/L.

Results and discussion

Figs. 1 and 2 show the variations in Se(VI) removal over time with Fe^{2+}-doped Mg-Al LDH and Mg-Al LDH. The molar ratios of Al in the LDH to Se(VI) in the solution (Al/Se molar ratios) were set at 1 to 3. For both LDHs, Se(VI) removal increased with time for all Al/Se molar ratios, showing that the LDHs could remove Se(VI) from aqueous solution. The Se(VI) removal also increased with increasing Al/Se molar ratios, indicating that increased amounts of LDH resulted in increased uptake of Se(VI). This was caused by the increase of adsorption site for Se(VI). However, Se(VI) removal for the Fe^{2+}-doped Mg-Al LDH was consistently larger than that for the undoped Mg-Al

LDH when Al/Se = 1 and 2. This implies the activity of the Fe^{2+} as a reducing agent, and is discussed later. When Al/Se = 3, the Se(VI) removal by Fe^{2+}-doped Mg-Al LDH was almost the same as that by undoped Mg-Al LDH, suggesting that the amount of undoped LDH was sufficiently high to remove Se(VI) even without the activity of the Fe^{2+}. The Fe^{2+}-doped Mg-Al LDH had a great advantage in Se(VI) removal when Al/Se = 1 and 2.

Fig. 3 shows the XRD patterns for the Fe^{2+}-doped Mg-Al LDH and undoped Mg-Al LDH before and after Se(VI) removal. The XRD peaks for all samples were assigned to hydrotalcite (JCPDS card 22-700), a naturally occurring hydroxycarbonate of magnesium and aluminum with the formula $Mg_6Al_2(OH)_{16}CO_3 \cdot 4H_2O$ and structure of a LDH, proving that all samples had the basic LDH structure. The presence of hydrotalcite suggests that the removal of Se(VI) from aqueous solution by the LDHs is due to anion exchange, that is, the intercalation of SeO_4^{2-} into the interlayers of the LDH. The XRD patterns for Fe^{2+}-doped Mg-Al LDH and undoped Mg-Al LDH after Se(VI) removal (Figs. 3(b) and 3(d)) display (003) reflections corresponding to the basal spacing of the LDH that are broader and weaker than those before Se(VI) removal (Figs. 3(a) and 3(c)). These reflections are likely attributable to the structural disorganization that arises from the intercalation of SeO_4^{2-}, which has a sterically bulky molecular structure. For undoped Mg-Al LDH, the basal spacing (d_{003}) increased from 8.1 Å to 8.3 Å upon the removal of

Se(VI) (Figs. 3(c) and 3(d)), which confirms anion exchange occurred between Cl^- intercalated in the interlayer of the Mg-Al LDH and SeO_4^{2-} in the aqueous solution. On the other hand, for Fe^{2+}-doped Mg-Al LDH, the basal spacing (d_{003}) decreased from 8.1 Å to 7.8 Å upon the removal of Se(VI) (Figs. 3(a) and 3(b)). Table 1 shows the oxidation states of Fe and Se in the Fe^{2+}-doped Mg-Al LDH after removal of Se(VI). It was found that Fe^{2+} was oxidized to Fe^{3+} and Se(VI) was reduced to Se(IV). Therefore, the decrease in basal spacing (d_{003}) for the Fe^{2+}-doped Mg-Al LDH is attributed to the intercalation of SeO_3^{2-}, which has a smaller ionic radius than SeO_4^{2-}. Thus, the increased Se(VI) removal by the Fe^{2+}-doped Mg-Al LDH compared with the undoped Mg-Al LDH is attributed to the increased charge density of SeO_3^{2-}, which is more easily exchanged with intercalated Cl^- than SeO_4^{2-}.

The schematic diagram for Se(VI) removal by the Fe^{2+}-doped Mg-Al LDH is shown in Fig. 4. The Fe^{2+}-doped Mg-Al LDH adsorbs Se(VI) as SeO_4^{2-} from an aqueous solution through anion exchange with intercalated Cl^-. Se(VI) is reduced to Se(IV) upon oxidation of Fe^{2+} to Fe^{3+} in the LDH host layer, and the Se(IV) produced as SeO_3^{2-} is again adsorbed by the Fe^{2+}-doped Mg-Al LDH through anion exchange with intercalated Cl^-. Se(IV) adsorption does not occur in undoped Mg-Al LDH as only SeO_4^{2-} is adsorbed by this structure. The reduction of Se(VI) to Se(IV) is advantageous for Se(VI) removal by the Fe^{2+}-doped Mg-Al LDH due to the increased charge density of SeO_3^{2-}. The Fe^{2+}-doped Mg-Al LDH can effectively remove Se(VI) from an aqueous solution because of anion exchange properties of the LDH and activity of Fe^{2+} as a reducing agent.

Fig. 5 shows the adsorption isotherm of Se(VI) adsorbed by the Fe^{2+}-doped Mg-Al LDH where the equilibrium adsorption increased rapidly with increasing equilibrium concentration. The adsorption isotherm showed Langmuir-type behavior, which was confirmed by arranging the experimental data according to the Langmuir equation, expressed as

$$q_e = C_e q_m K_L/(1 + C_e K_L), \qquad (1)$$

where q_e (mmol g^{-1}) is the equilibrium adsorption, C_e (mM) is the equilibrium concentration, q_m (mmol g^{-1}) is the maximum adsorption, and K_L is the equilibrium adsorption constant. This equation can also be expressed as

$$C_e/q_e = 1/q_m K_L + C_e/q_m. \qquad (2)$$

Fig. 6 shows plots of C_e/q_e versus C_e for the adsorption isotherm of Se(VI) adsorbed by the Fe^{2+}-doped Mg-Al LDH. The high linearity indicates that this process follows a Langmuir-type adsorption. The values of q_m and K_L, determined from the slope and intercept of the straight line in Fig. 6, were 1.4 mmol g^{-1} and 1.6, respectively.

Fig. 7 shows the variations in Se(VI) removal by the Fe^{2+}-doped Mg-Al LDH over time at various temperatures. Se(VI) removal increased with time and increasing the temperature from 10 to 30 °C, but was almost constant when the temperature increased from 30 to 60 °C. These results suggest that higher temperatures enhance chemical adsorption (*i.e.* anion exchange of SeO_4^{2-} and SeO_3^{2-} with intercalated Cl^-).

Next, the kinetics of Se(VI) removal by the Fe^{2+}-doped Mg-Al LDH were examined based on the data shown in Fig. 7. First-order kinetics, which depend on the concentration of Se(VI), may be expressed by

$$-\ln(1-x) = kt, \tag{3}$$

where x is the degree of Se(VI) removal, t (min) is the reaction time, and k (min^{-1}) is the rate constant for Se(VI) removal. Fig. 8 presents the first-order plots of Se(VI) removal at various temperatures. None of the plots show good linearity, regardless of temperature, indicating that Se(VI) removal cannot be represented by first-order reaction kinetics. Thus, pseudo second-order kinetics may be expressed by [20–22]

$$\mathrm{d}q_t/\mathrm{d}t = k(q_e - q_t)^2 \tag{4}$$

where q_t (mmol g^{-1}) is the amount of Se(VI) removed at reaction time t, q_e (mmol g^{-1}) is the amount of Se(VI) removed at equilibrium, and k (g $mmol^{-1}$ min^{-1}) is the rate constant for Se(VI) removal. Integration of Eq. (4) gives

$$t/q_t = 1/(kq_e^2) + t/q_e. \tag{5}$$

The pseudo second-order reaction can predict the adsorption behavior by assuming that the rate-determining step consists of chemical adsorption involving valence forces through the sharing or exchange of electrons between the adsorbent and adsorbate.[20,21,23–25] Fig. 9 displays the pseudo second-order plot for Se(VI) removal at various temperatures, which shows good linearity at all temperatures and confirms that Se(VI) removal can be represented by pseudo second-order reaction kinetics. The apparent rate constants at 10, 30, and 60 °C were 1.2×10^{-3}, 1.5×10^{-3}, and 2.2×10^{-3} g mmol^{-1} min^{-1}, respectively. Thus, the apparent rate constant clearly increased with increasing temperature. An Arrhenius plot of the rate constants, determined from the slopes of the lines in Fig. 9, is shown in Fig. 10 and yields an apparent activation energy of 10.0 kJ mol^{-1}.

There are two main types of adsorption: physical and chemical. Typically, the forces involved in physical adsorption are weak and have activation energies of no more than 4.2 kJ mol^{-1}. Chemical adsorption, however, is highly specific and involves forces much stronger than those in physical adsorption. With chemical adsorption, the reaction rate varies with temperature according to a finite activation energy (8.4–83.7 kJ mol^{-1}) in the Arrhenius equation.[25–27] The apparent activation energy of 10.0 kJ mol^{-1} for Se(VI) removal is within the finite activation energy range of chemical adsorption. Therefore, this result confirms that the rate-determining step in Se(VI) removal by the Fe^{2+}-doped Mg-Al LDH is chemical adsorption involving anion exchange of SeO_4^{2-} and SeO_3^{2-} with intercalated Cl^- and that Se(VI) removal is well expressed as a pseudo second-order reaction.

Conclusions

The Se(VI) removal efficiencies of undoped and Fe^{2+}-doped Mg-Al LDH were compared in this study, and the latter was proved to be superior. Both LDHs adsorbed Se(VI) as SeO_4^{2-} through anion exchange with intercalated Cl^-. However, in the Fe^{2+}-doped Mg-Al LDH, Se(VI) was reduced to Se(IV) upon oxidation of Fe^{2+} to Fe^{3+} in LDH host layer. Se(IV), available as SeO_3^{2-}, was also adsorbed by the Fe^{2+}-doped Mg-Al LDH through anion exchange. Reduction of Se(VI) to Se(IV) is advantageous for Se(VI) removal by the Fe^{2+}-doped Mg-Al LDH due to the increased charge density of SeO_3^{2-}. The Fe^{2+}-doped Mg-Al LDH could remove Se(VI) effectively from an aqueous solution because of the anion exchange properties of the LDH and activity of the Fe^{2+} as a reducing agent. This process was considered to occur through Langmuir-type adsorption, where the maximum adsorption and equilibrium adsorption constant were 1.4 mmol g^{-1} and 1.6, respectively. Se(VI) removal could be well expressed as a pseudo second-order reaction. The apparent rate constants at 10, 30, and 60 °C were 1.2×10^{-3}, 1.5×10^{-3}, and 2.2×10^{-3} g $mmol^{-1}$ min^{-1}, respectively, and the apparent activation energy was 10.0 kJ mol^{-1}. The rate-determining step in Se(VI) removal by the Fe^{2+}-doped Mg-Al LDH was confirmed to be chemical adsorption involving anion exchange of SeO_4^{2-} and SeO_3^{2-} with intercalated Cl^{-}.

Acknowledgments

This research was partially supported by the Ministry of Education, Science, Sports, and Culture, Grant-in-Aid for Challenging Exploratory Research, 23651061, 2011-2013.

References

1 F. Cavani, F. Trifiro, A. Vaccari, *Catal. Today*, 1991, **11**, 173.

2 L. Ingram, H.F.W. Taylor, *Mineral. Mag.*, 1967, **36**, 465.

3 R. Allmann, *Acta Cryst.*, 1968, **B24**, 972.

4 S.J. Mills, A.G. Christy, J-M.R. Genin, T. Kameda, F. Colombo, *Mineral. Mag.*, 2012, **76**, 1289.

5 K.-H. Goh, T.-T. Lim, Z. Dong, *Water Res.*, 2008, **42**, 1343.

6 S. Mandal, S. Mayadevi, B.D. Kulkarni, *Ind. Eng. Chem. Res.*, 2009, **48**, 7893.

7 X. Wu, X. Tan, S. Yang, T. Wen, H. Guo, X. Wang, A. Xu, *Water Res.*, 2013, **47**, 4159.

8 A.G. Caporale, M. Pigna, S.M.G.G. Azam, A. Sommella, M.A. Rao, A. Violante, *Chem. Eng. J.*, 2013, **225**, 704.

9 D. Kovacevic, B.N. Dzakula, D. Hasenay, I. Nemet, S. Roncevic, I. Dekany, D. Petridis, *Croat. Chem. Acta*, 2013, **86**, 273.

10 X. Yuan, Y. Wang, J. Wang, C. Zhou, Q. Tang, X. Rao, *Chem. Eng. J.*, 2013, **221**, 204.

11 S. Kaneko, M. Ogawa, *Appl. Clay Sci.*, 2013, **75–76**, 109.

12 S. Paikaray, M.J. Hendry, *Appl. Clay Sci.*, 2013, **77–78**, 33.

13 S. Paikaray, M.J. Hendry, J.E.Dughan, *Chem. Geology*, 2013, **345**, 130.

14 T. Kameda, M. Honda, T. Yoshioka, *Sep. Purif. Technol.*, 2011, **80**, 235.

15 T. Kameda, M. Nakamura, T. Yoshioka, *J. Environ. Sci. Health Part A*, 2012, **47**, 1146.

16 T. Kameda, M. Nakamura, T. Yoshioka, *Fresenius Environ. Bull.*, 2012, **21**, 1323.

17 D. H. K. Reddy, S.-M. Lee, *Adv. Colloid Interface*, 2013, **201-202**, 68.

18 T. Kameda, E. Kondo, T. Yoshioka, *Sep. Purif. Technol.*, 2014, **122**, 12.

19 Sangyou Kanri Kyoukai, Shin Kougai Boushi no Gijyutsu to Houki 2011, Suishitsu hen II, Maruzen, Tokyo, 2011.

20 Y.S. Ho, G. McKay, *Process Biochem.*, 1999, **34**, 451.

21 Y.S. Ho, *J. Hazard Mater.*, 2006, **B136**, 681.

22 F.C. Wu, R.L. Tseng, S.C. Huang, R.S. Juang, *Chem. Eng. J.*, 2009, **151**, 1.

23 Z.P. Liang, Y.Q. Feng, Z.Y. Liang, S.X. Meng, *Biochem. Eng. J.*, 2005, **24**, 65.

24 Z.P. Liang, Y.Q. Feng, S.X. Meng, Z.Y. Liang, *Process Biochem.*, 2005, **40**, 3218.

25 M. Kragovic, A. Dakovic, M. Markovic, J. Krstic, G.D. Gatta, N. Rotiroti, *Appl. Surface Sci.*, 2013, **283**, 764.

26 Z. Aksu, *Process Biochem.*, 2002, **38**, 89.

27 W. Zou, R. Han, Z. Chen, Z. Jinghua, *J. Colloids Surf. A Physicochem. Eng. Aspects*, 2006, **279**, 238.

Figure legends

Fig.1

Variations in Se(VI) removal over time by the Fe^{2+}-doped Mg-Al LDH with various molar ratios of Al in the LDH to Se(VI) in solution at 30 ºC.

Fig. 2.

Variations in Se(VI) removal over time by the undoped Mg-Al LDH with various molar ratios of Al in the LDH to Se(VI) in solution at 30 ºC.

Fig. 3.

XRD patterns for the Fe^{2+}-doped Mg-Al LDH (a) before and (b) after Se(VI) removal and undoped Mg-Al LDH (c) before and (d) after Se(VI) removal.

Fig. 4.

Schematic diagram for Se(VI) removal by the Fe^{2+}-doped Mg-Al LDH.

Fig. 5.

Adsorption isotherm of 0.5–25 mM Se(VI) adsorbed by 0.2 g Fe^{2+}-doped Mg-Al LDH at

30 ºC after 24 h.

Fig. 6.

Plots of C_e/q_e versus C_e for the adsorption isotherms of 0.5–25 mM Se(VI) adsorbed by 0.2 g Fe^{2+}-doped Mg-Al LDH at 30 ºC after 24 h.

Fig. 7.

Variations in Se(VI) removal by the Fe^{2+}-doped Mg-Al LDH over time at various temperatures for Al/Se = 1.

Fig. 8.

First-order plot of Se(VI) removal by the Fe^{2+}-doped Mg-Al LDH at various temperatures.

Fig. 9.

Pseudo second-order plot of Se(VI) removal by the Fe^{2+}-doped Mg-Al LDH at various temperatures.

Fig. 10.

Arrhenius plot of the apparent rate constant of Se(VI) removal by the Fe^{2+}-doped Mg-Al LDH.

Table captions

Table 1

Oxidation states of Fe and Se in Fe^{2+}-doped Mg-Al LDH after removal of Se(VI).

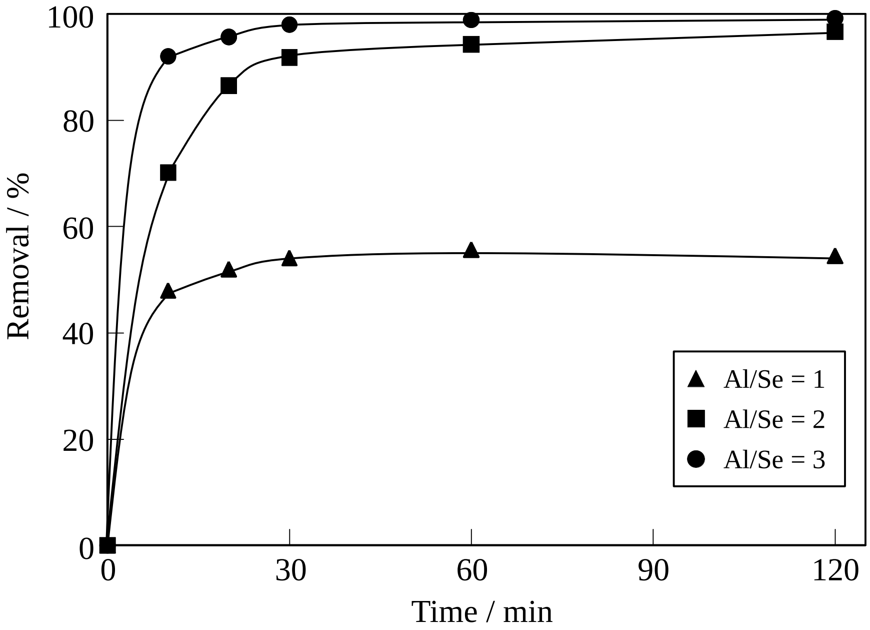

Fig.1 Variations in Se(VI) removal over time by the Fe^{2+}-doped Mg-Al LDH with various molar ratios of Al in the LDH to Se(VI) in solution at 30 ºC.

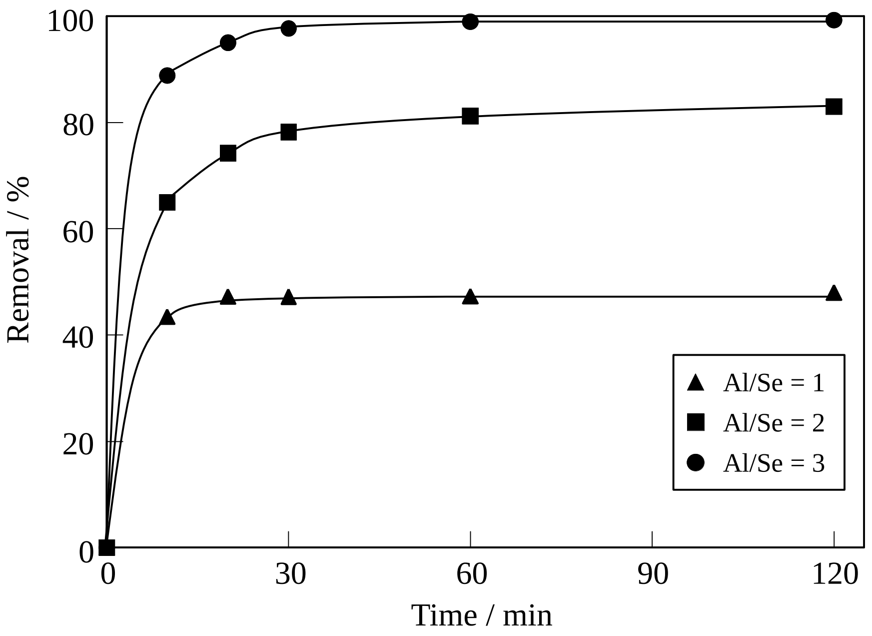

Fig.2 Variations in Se(VI) removal over time by the undoped Mg-Al LDH with various molar ratios of Al in the LDH to Se(VI) in solution at 30 ºC.

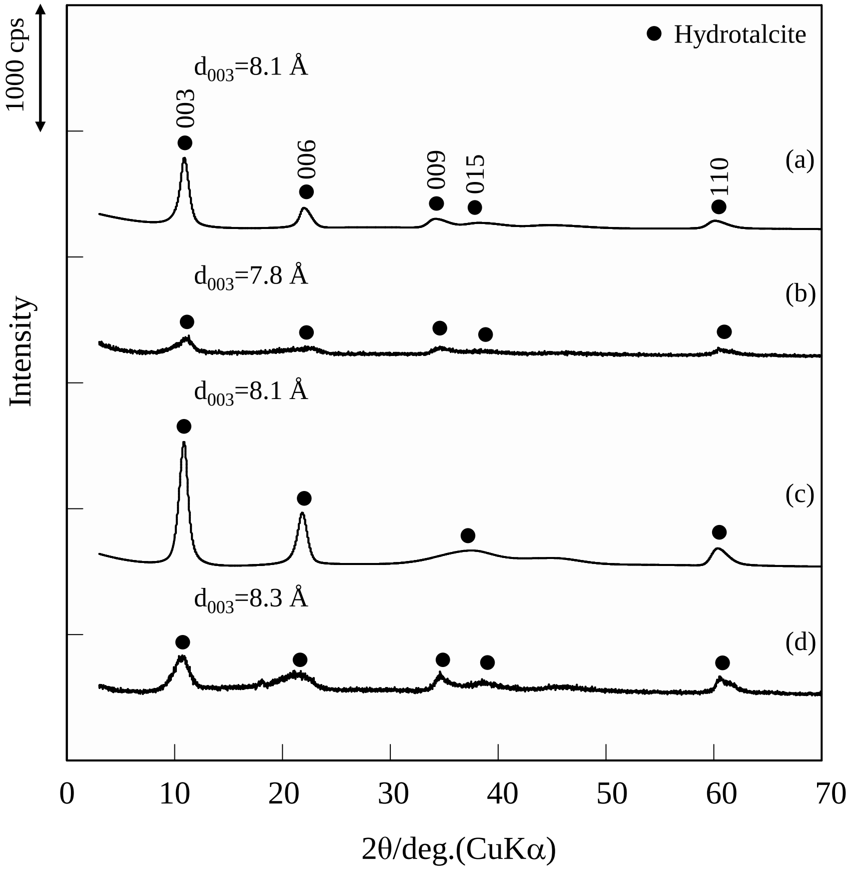

Fig.3 XRD patterns for the Fe^{2+}-doped Mg-Al LDH (a) before and (b) after Se(VI) removal and undoped Mg-Al LDH (c) before and (d) after Se(VI) removal.

Table 1 Oxidation states of Fe and Se in Fe^{2+}-doped Mg-Al LDH after removal of Se(VI).

Fe^{2+}/Fe	Fe^{3+}/Fe	Se(IV)/Se	Se(VI)/Se
0	1	0.69	0.31

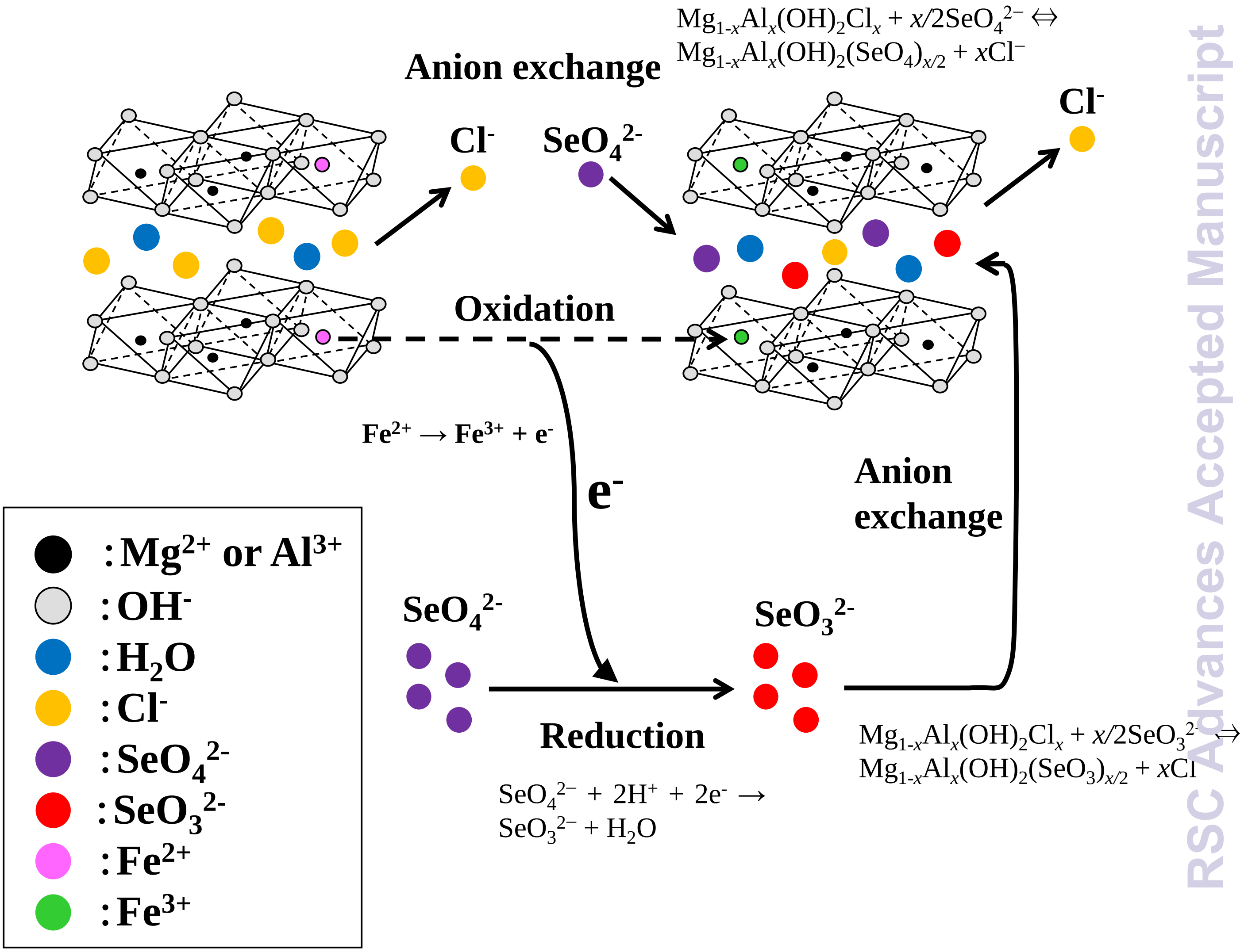

Fig.4 Schematic diagram for Se(VI) removal by the Fe^{2+}-doped Mg-Al LDH.

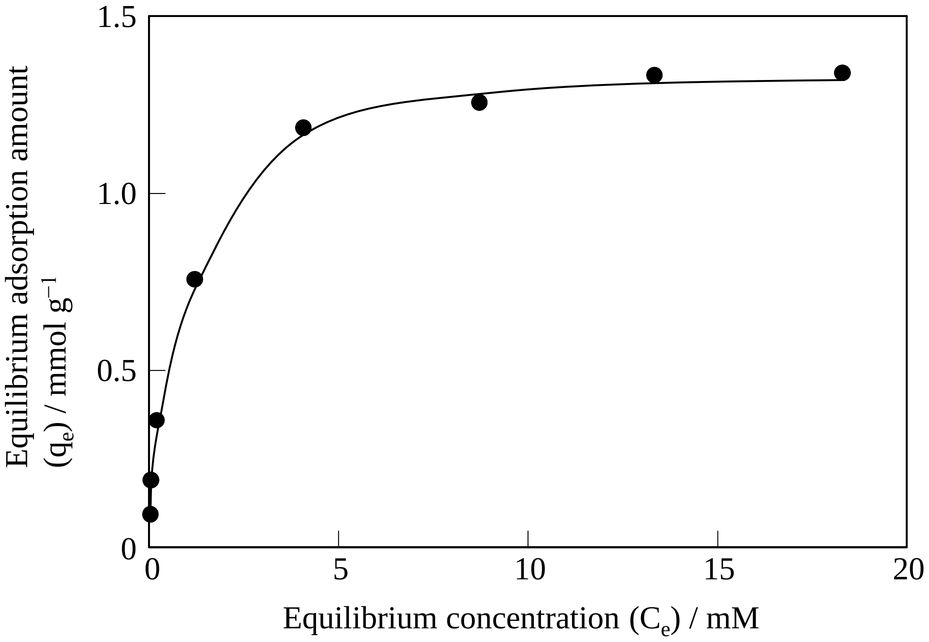

Fig.5 Adsorption isotherm of 0.5–25 mM Se(VI) adsorbed by 0.2 g Fe^{2+}-doped Mg-Al LDH at 30 ºC after 24 h.

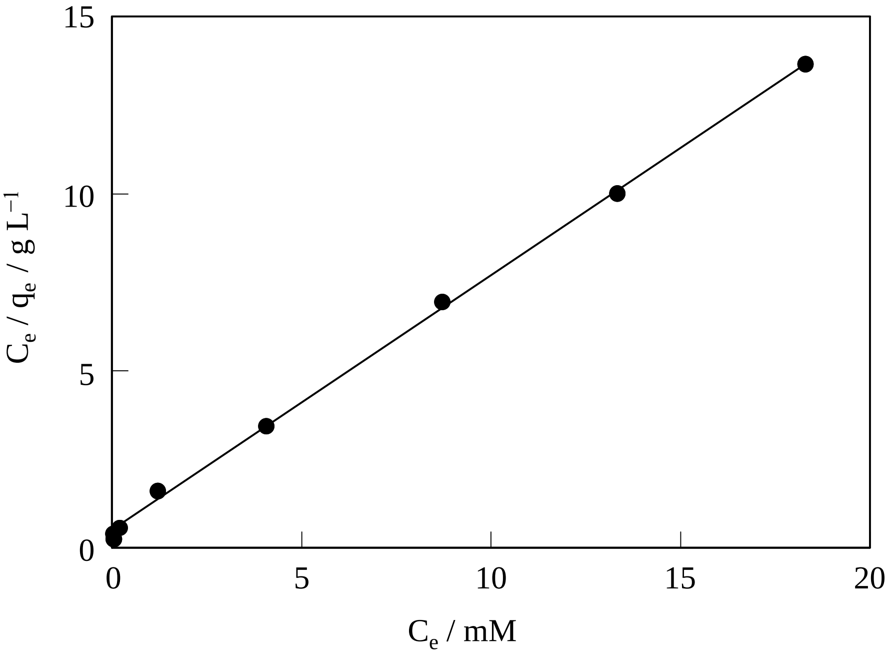

Fig.6 Plots of C_e/q_e versus C_e for the adsorption isotherms of 0.5–25 mM Se(VI) adsorbed by 0.2 g Fe^{2+}-doped Mg-Al LDH at 30 ºC after 24 h.

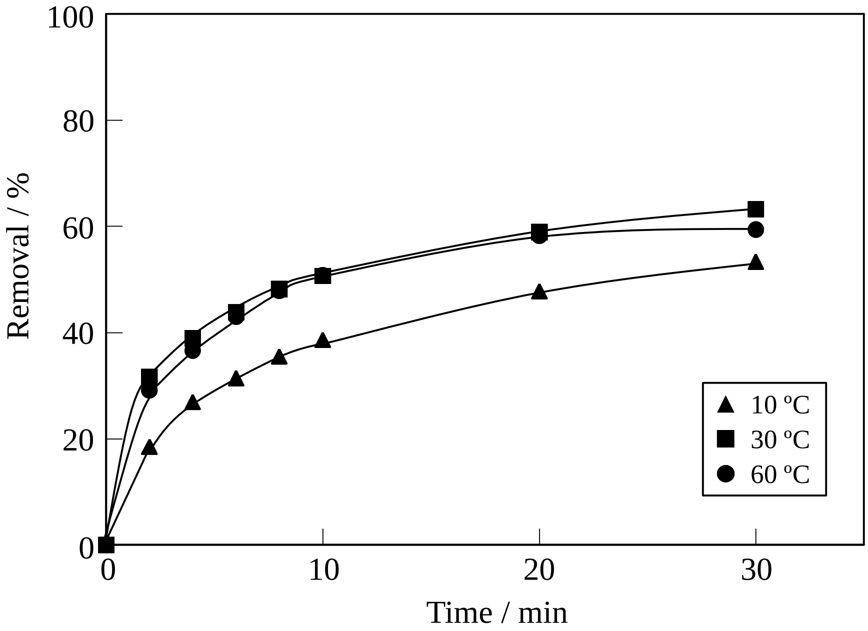

Fig.7 Variations in Se(VI) removal by the Fe^{2+}-doped Mg-Al LDH over time at various temperatures for Al/Se = 1.

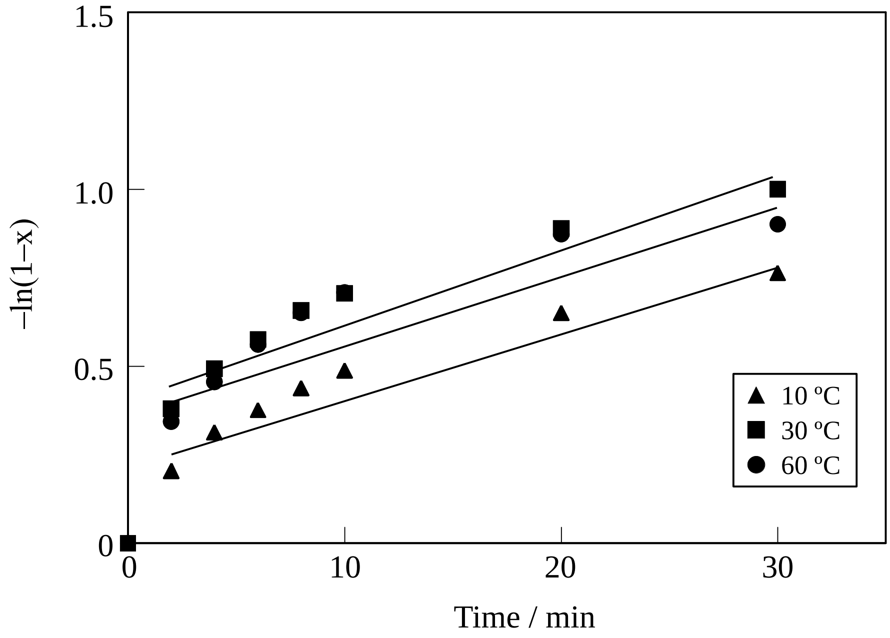

Fig.8 First-order plot of Se(VI) removal by the Fe^{2+}-doped Mg-Al LDH at various temperatures.

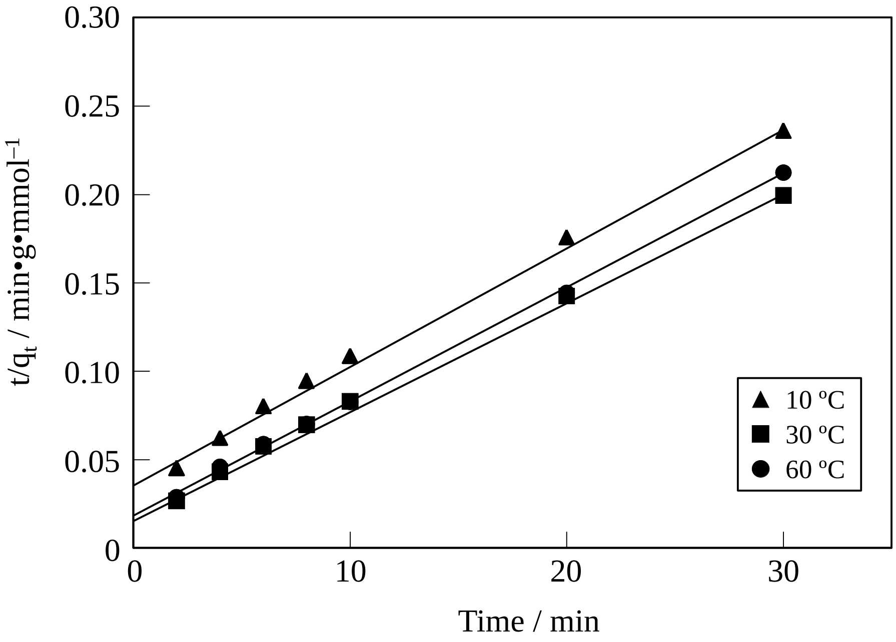

Fig.9 Pseudo second-order plot of Se(VI) removal by the Fe^{2+}-doped Mg-Al LDH at various temperatures.

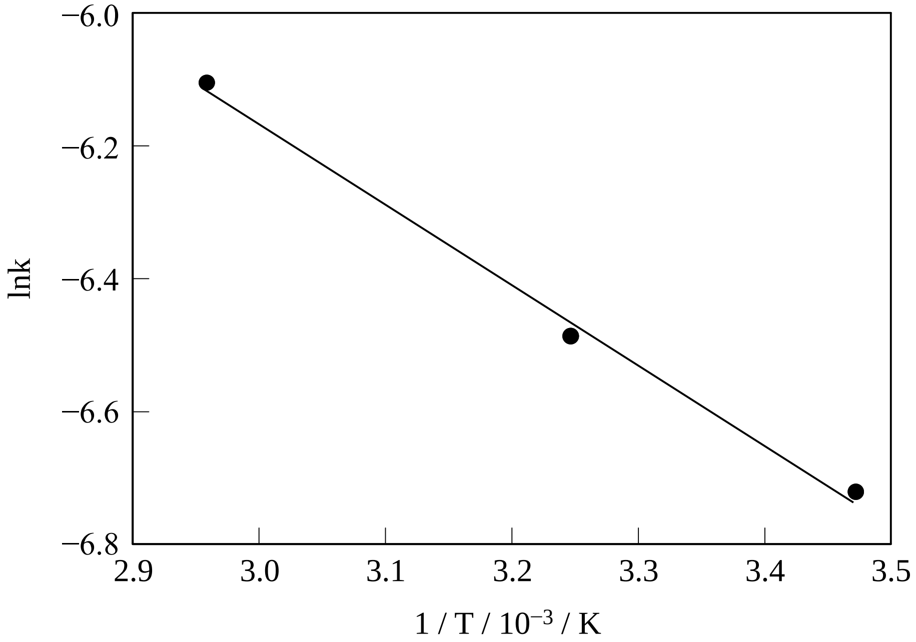

Fig.10 Arrhenius plot of the apparent rate constant of Se(VI) removal by the Fe^{2+}-doped Mg-Al LDH.